Stark broadening of the He I 4471-Å line and its forbidden component in dense cool plasma

N. I. Uzelac and N. Konjević
Institute of Physics, P.O. Box 57, 11001 Beograd, Yugoslavia
(Received 8 July 1985)

We have measured the profile of the He I 4471-Å line and its forbidden component at 4470 Å in the plasma of a high-pressure pulsed discharge at an electron temperature of about 1.5 eV, and at electron densities ranging from 0.5×10^{17} to 2.0×10^{17} cm^{-3}. Contrary to all preceding experiments performed at higher electron temperatures, in the present experiment better agreement with theoretical calculations is found. A tentative explanation of this improved agreement is offered.

I. INTRODUCTION

The Stark broadening of the He I 4471-Å (2^3P-4^3D) line and its forbidden component (2^3P-4^3F) has attracted considerable interest for several reasons. First, the lines appear in the spectra of B-type stars[1,2] and are important in model-atmosphere calculations. Second, the shape of these lines is very sensitive to the variations in charged-particle densities and therefore can be very useful in astrophysical and laboratory plasma diagnostics. Finally, the comparison of the overall experimental profiles of these lines with the results of theoretical calculations may be used as a sensitive test of Stark-broadening theories.

Most of the experimental work was devoted to the study of the He I 4471-Å line shapes at relatively low electron densities $N_e<1\times10^{16}$ cm^{-3} (see, e.g., Ref. 3 and references therein).

Nevertheless, in many laboratory plasmas at higher electron densities $N_e>1\times10^{16}$ cm^{-3} this line is also interesting for plasma diagnostic purposes. In this case the forbidden component becomes as intense as the allowed line, and the broadening of the combined lines should then be described by hydrogenic calculations similar to H_β. Detailed comparison of computed and measured line profiles may provide a very sensitive test of modern line-broadening theories.

We shall limit the following discussion to the experimental and theoretical studies which cover the broadening of the He I 4471-Å line and its forbidden component at high electron densities, $N_e>5\times10^{16}$ cm^{-3}. There are several experimental papers[4-9] which report Stark profiles of this line at high electron densities. They are listed in Table I where one can find all essential information about the plasma sources and methods used for independent plasma diagnostics. The range of plasma parameters achieved in these experiments is given in the last two columns of Table I. With the exception of Ref. 5, all experimental results were compared with theoretical calculations by Griem[10] and by Barnard *et al.*[11] The authors of Ref. 5 compared the results only with their own calculations which were in close agreement with the preceding two.[10,11] In addition to Refs. 10 and 11, the authors of Ref. 6 used for comparison the theoretical calculations by Deutsch *et al.*[12] which are, unfortunately, limited to electron densities below 5×10^{16} cm^{-3}.

Detailed comparison between the experiments[4-9] and theoretical calculations[10,11] (see also Figs. 1—4) shows the following.

(a) Both sets of total half-width $\Delta\lambda_{1/2}$ data (see Fig. 5 for definition and notation) agree within the estimated errors of both theory and experiment.

(b) Discrepancies between theory and experiment for the separation of the peaks of allowed and forbidden component $\Delta\lambda_{AF}$, the ratio of the peak intensities I_F/I_A, and the ratio of the valley to the peak intensity of allowed component I_V/I_A exceed the estimated uncertainties.

(c) Large discrepancies between various experimental results exist.

Contrary to all other experimental data, the measurements of Ref. 5 are in fairly good agreement with theory.[5] The only exception is the measurement at $N_e=1.6\times10^{17}$ cm^{-3} where a significant difference between theory and experiment in the central part between two line profiles is detected [see Fig. 2(b) in Ref. 5].

Here one should note that all the experiments quoted in Table I could be divided into two groups. In one of them Stark profiles were recorded at relatively high electron temperatures, 4—5 eV,[4,8,9] while the rest of the data were measured at ~2 eV.[5-7] Nelson and Barnard[4] offered a tentative explanation for the discrepancy between their experimental data and theory[10,11] (see in particular the comparison of shift measurements in Fig. 2), and this explanation may be applied to the rest of the high-temperature data.[8,9] They[4] point out that in the calculations of Stark profiles of the He I 4471-Å line and its forbidden component, the ion field distribution for singly charged ions was used.[10,11] Actually, at the high temperatures of their pulsed arc[4] the fraction of doubly ionized helium atoms becomes appreciable. The doubly charged ions have two effects on the ion field distribution: (1) The Holtsmark normal field strength becomes larger than the field for plasmas with only singly charged ions at the same electron density, but (2) the field distribution function will also be changed because correlations are more important

TABLE I. Key data on experiments.

Authors	Plasma source	Plasma diagnostics	Plasma parameters: Temperature	Plasma parameters: Electron density (10^{17} cm^{-3})
Nelson and Barnard (Ref. 4)	Low-pressure pulsed arc	T_e: ratio of He II 4686 to He I 5876 Å N_e: He I 3889 Å	4.5 eV	0.3–1.1
Greig *et al.* (Ref. 5)	T tube	T_e: ratio of He I lines and continuum N_e: continuum at 6678 Å, Stark widths of 4471- and 6678-Å He I lines	25 000 K	1.6–4.4
Hawryluk *et al.* (Ref. 6)	CO_2 laser-produced plasma	T_e: ratio of He II 4686 to He I 5876 Å and line to continuum ratio for He I 6678 and 4713 Å N_e: Stark widths of He II 4686 and He I 4713 Å	20 000 K	0.2–1.2
Hey and Griem (Ref. 7)	T tube	T_e: ratios of He I lines to continuum N_e: Stark widths of H_β, He I 6678 and 3889 Å and absolute continuum of 5400 Å	16 500–18 000 K	0.8–1.4
Baravian *et al.* (Ref. 8)	Nd:glass laser-produced plasma	T_e: ratios of He I 5876-, 5015-, 4922-, and 4471-Å lines to continuum N_e: Stark widths of He I 3889 and 5015 Å	3–4 eV	0.2–1.8
Vujičić and Ćirković (Ref. 9)	CO_2 laser-produced plasma	T_e: ratios of He I lines 5876 and 4471 Å to the continuum and ratio of He II 4686 to He I 5876 Å N_e: Stark widths of He II 4686 and He I 3889 and 4713 Å	42 000–55 000 K	0.2–1.3

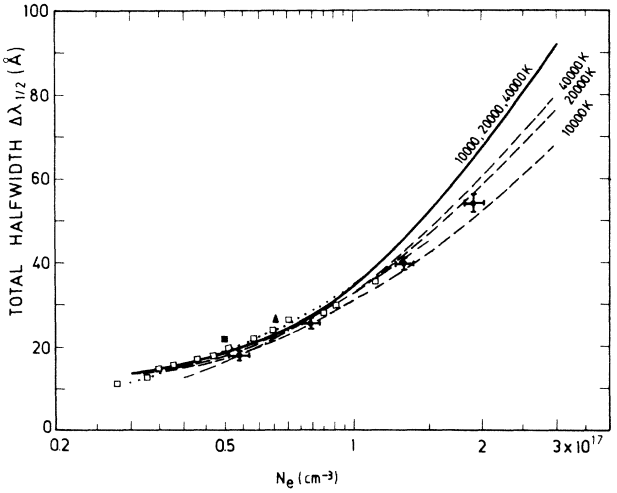

FIG. 1. Total half-width of 4471-Å profile as a function of electron density. Solid and dashed lines, computed values from Griem (Ref. 10) and Barnard *et al.* (Ref. 11), respectively. Experiments: dotted and dot-dashed lines, best-fit data from Nelson and Barnard (Ref. 4) and Baravian *et al.* (Ref. 8), respectively; ■, Hawryluk *et al.* (Ref. 6); ▲, Hey and Griem (Ref. 7); □, Vujičić and Ćirković (Ref. 9); ⊢⊣, this experiment with estimated error bars.

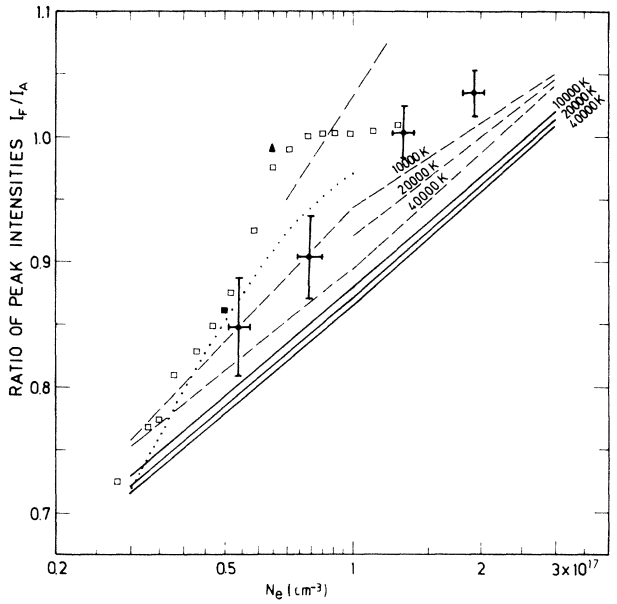

FIG. 3. Ratio of intensities of forbidden I_F to the intensity of allowed line I_A vs electron density. For notation see caption of Fig. 1.

for doubly charged ions. Although it was not possible to say without detailed calculations whether the latter effect will completely offset the increased scaling factor, in Ref. 4 the authors suggest that the smaller ion field would be more probable, and as a result the shifts would be reduced. This explanation could also be given for the other high-temperature experiments.[8,9] Furthermore, in Ref. 4 the simplifications introduced in the computations[10,11] of line shifts by limiting the number of perturbing levels to those with the same principal quantum number n as the upper level were examined. It has been suggested[4] that the energy levels with $n=5$ may be important since one could expect them to depress the $4F$ levels more than $4D$ levels and in this way reduce the separation between the allowed and forbidden component.

If the idea of the possible influence of ion field distribution is applied to the line shifts,[4] the experiments performed at lower electron temperatures[5–7] should be in better agreement with theory[10,11] than one can detect in Figs. 1–4.

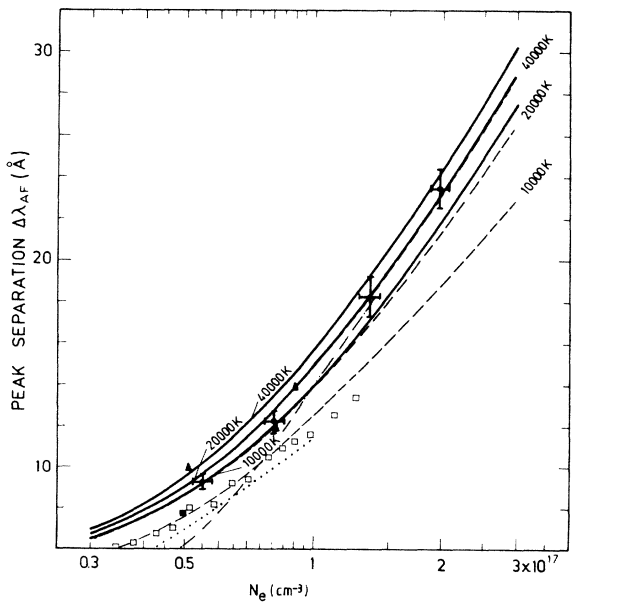

FIG. 2. Separation $\Delta\lambda_{AF}$ between allowed and forbidden components as a function of electron density. For notation see caption of Fig. 1.

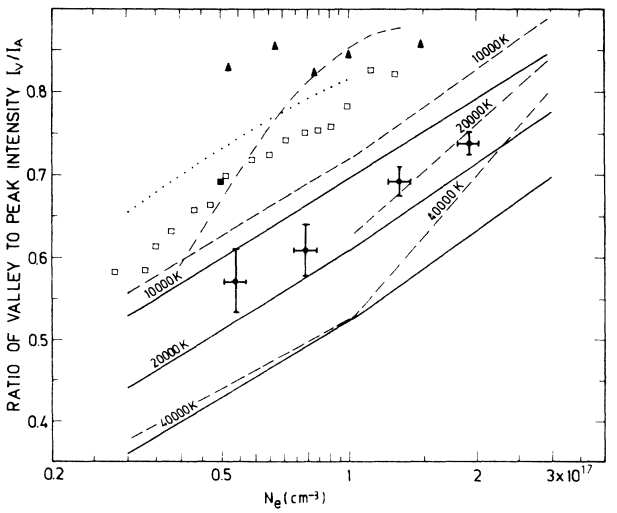

FIG. 4. Ratio of valley I_V to allowed line intensity I_A vs electron density. For notation see caption of Fig. 1.

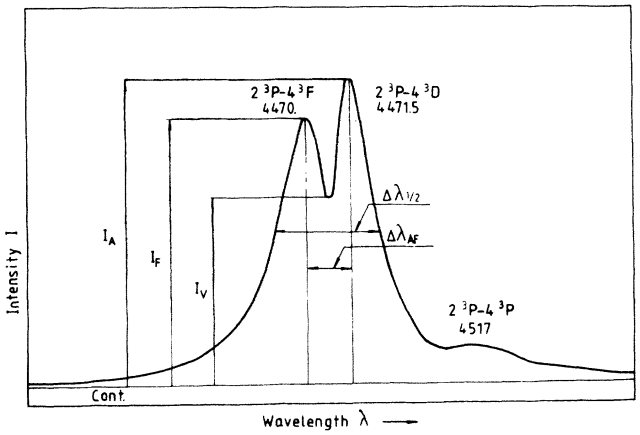

FIG. 5. He I 4471-Å profile for 1×10^{17} electrons/cm^3 and $T=20000$ K calculated by Griem (Ref. 10), illustrating the parameters $\Delta\lambda_{1/2}$, $\Delta\lambda_{AF}$, I_A, I_F, and I_V.

In order to clear up this puzzling discrepancy between theory and experimental data we set up a new experiment where the line shapes of the He I 4471-Å line are measured in a dense, cool helium plasma with negligible concentration of doubly ionized helium atoms. In this way we intended to approach plasma conditions assumed in theoretical calculations.[10,11] Special attention is paid to all the effects which may influence the line-shape measurements such as self-absorption, plasma instabilities, etc., while for line-spectra recordings we used a single-shot optical-multichannel method instead of the shot-by-shot technique.

II. APPARATUS AND EXPERIMENTAL PROCEDURE

A. Plasma source

In order to create a high density and relatively low electron temperature plasma, we used a high-pressure pulsed helium arc developed for this particular experiment (see Fig. 6). It consists of a quartz tube with a 4-mm internal diameter; the end parts of the tubing are supplied with quartz rods optically polished at both sides so that they are used as windows for end-on plasma observations and axial electron density measurements. Thoriated tungsten electrodes are located side on (see Fig. 6), behind the optical surfaces of quartz rods which in this way are protected from the deposition of electrode materials. This made it possible that a single pulsed arc would be used for more than 1000 shots. The lifetime of the helium pulsed arc depended critically upon the heat and vacuum treatment of the glass tubing and electrodes which preceded the filling of the device with 400 mbar of research-grade helium.

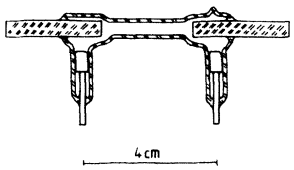

FIG. 6. Schematic diagram of the plasma source.

The discharge current was derived from a capacitor bank consisting of four 60-μF capacitors connected in parallel through a series of inductors (lumped delay line configuration). The charging voltage ranged between 0.6 and 1.1 kV. The current waveform approximated a square wave with a flat part lasting about 800 μs and current densities ranging from 1.1 to 2.8 kA/cm^2. The impedance of the electrical circuitry was such that it was possible to achieve a critically damped discharge, which simplified the application of laser interferometry for electron density diagnostics. In order to start the discharge it was necessary to apply a high-voltage pulse to the electrodes. For this purpose a 0.33-μF capacitor was charged up to 9 kV. The initiation of the discharge was achieved by discharging this high-voltage capacitor through the discharge tube using a hydrogen thyratron as a switch. The initiation pulse was followed by the main current pulse obtained by discharging a capacitor bank through the discharge tube via an ignitron.

B. Plasma spectroscopy

The light observed end on from the plasma axis of the pulsed arc was directed by f/100 collection optics into the entrance slit a 0.3-m McPherson or 1-m Spex grating monochromator with inverse linear dispersion of 26.5 and 7.6 Å/mm, respectively. At the place of the exit-slit assembly an optical-multichannel analyzer (OMA 2, Princeton Applied Research) is mounted in order to be used for single-pulse line-spectra recording. This OMA has a 12.5-mm-wide photodiode divided into 500 channels. An effective spectral resolution of 0.7 and 0.2 Å per channel was obtained. The channel-to-channel intensity calibration was obtained using a standard tungsten coiled-coil quartz-iodine lamp. The image intensifier was gated between 2 and 20 μs during the flat region of the current pulse, about 750 μs after the initiation of the discharge. The electron density remained constant during this period of time. The signal from the OMA 2 was digitized and transferred to a minicomputer for analysis. Complete line spectra could be analyzed on a single-shot basis. Two examples of spectra recordings are given in Fig. 7.

The contributions of the instrumental, Doppler, and van der Waals broadening to the He I 4471-Å line-shape measurements were negligible. For example, the instrumental linewidth was of the order of 1.5 and 0.6 Å (depending upon the monochromator), the Doppler linewidth did not exceed 0.25 Å in all cases, and the estimated van der Waals widths were smaller than 0.2 Å, while the most narrow measured 4471-Å profile had a Stark width of $\sim$15 Å.

Our main concern with the 4471-Å line-shape measurement was the possible distortion induced by the presence of self-absorption. In order to check this possibility experimentally we doubled the optical path length through

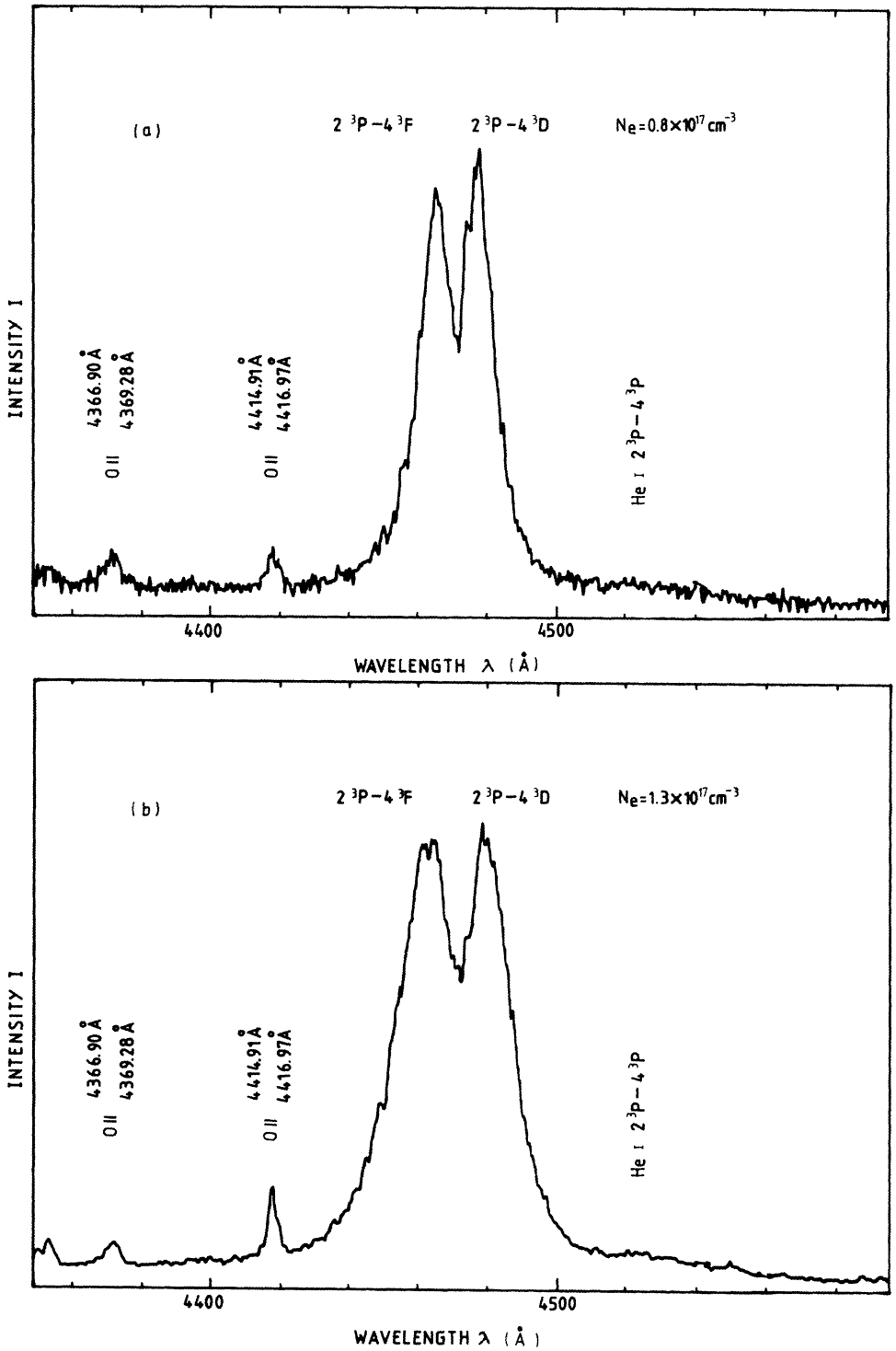

FIG. 7. Two typical spectral recordings of He I 4471-Å profile at two different electron densities: (a) 0.8×10^{17} cm^{-3} and (b) 1.3×10^{17} cm^{-3}.

the plasma by placing a concave mirror at a distance of two focal lengths behind the plasma. If this length increases, except for reflection and transmission losses, doubles the signal at the OMA along the whole profile of the investigated line, it would be an indication that self-absorption is not present. Here it should be pointed out that for each self-absorption check two separate plasma shots were necessary, one with and one without the mirror placed behind the plasma. Due to this procedure, the shot-to-shot plasma reproducibility made this test less reliable than, e.g., in the case of continuous plasma sources. Since this method is the only one which can be conveniently used for self-absorption checks in a helium plasma (for other techniques see, e.g., Ref. 13), we performed a large number of checks, which all indicated that the He I 4471-Å line was not distorted by any measureable absorp-

tion. As a matter of fact, except for the 5876-Å line, none of the visible He I lines showed any sign of self-absorption distortion under the studied experimental conditions.

C. Plasma diagnostics

The axial electron density was determined with a two-wavelength (6328 Å and 3.39 μm) He-Ne laser interferometer with a plane external mirror (see, e.g., Ref. 13). The electron temperatures were derived from the Boltzmann plot of the relative intensities of five O II impurity lines (4366.9, 4345.6, 4317.1, 4351.3, and 4347.4 Å), with the transition probabilities being taken from Ref. 14. Apart from O II impurity lines, Si II and Si III lines were also detected. There are several reasons why we have chosen those five O II lines. (1) All five selected lines are spectrally close enough so that only a single-shot experiment is required for temperature measurement. (2) Because of the small wavelength separation, the OMA monochromator system does not require spectral response calibration. (3) Transition probabilities are available for all five lines. (4) Self-absorption tests showed that all five lines were optically thin. The estimated error in the electron temperature measurements is within the range of $\pm 8\%$. The uncertainty of the electron density measurements does not exceed $\pm 10\%$ and is mainly due to uncertainties in the plasma length.

III. RESULTS AND DISCUSSION

All experimental results, i.e., plasma parameters, total half-widths $\Delta\lambda_{1/2}$, ratios of peak intensities of forbidden and allowed component I_F/I_A, and the separation between the peaks of the allowed and forbidden components $\Delta\lambda_{AF}$, are given in Table II together with the estimated uncertainties. The magnitude of the estimated errors listed in Table II illustrates the shot-to-shot reproducibility of plasma measurements much better than the actual error in measuring, e.g., the ratio of the valley to the peak intensity of the allowed component. In Figs. 1–4 the experimental results are compared with those of other experiments[4–9] and with theoretical calculations by Griem[10] and by Barnard *et al.*[11]

Comparison of the data in Figs. 1–4 shows the following.

(a) Total half-widths $\Delta\lambda_{1/2}$ (Fig. 1): Experimental data are in agreement with both calculations[10,11] at electron densities below 1×10^{17} cm^{-3}. At higher electron densities only the experimental results of Ref. 9 and our results are in close agreement with Barnard *et al.*[11]

(b) Peak separation $\Delta\lambda_{AF}$: Our experimental data are in very good agreement with the calculations by Griem[10] (Fig. 2). With the exception of the results by Hey and Griem,[7] all other experimental data are systematically lower than are the results of both this experiment and the theories.[10,11]

(c) Ratio of peak intensities I_F/I_A: Our experimental data are systematically lower than those of other experiments (Fig. 3). It is interesting, however, that at lower electron densities ($N_e < 0.5\times10^{17}$ cm^{-3}) the scatter of experimental data becomes smaller and the agreement with theory becomes better.

(d) Ratio of valley to peak intensity I_V/I_A: The largest discrepancy between our experiment and all other experimental data is noted here (Fig. 4). Our experiment is in good agreement with both sets of theoretical calculations.[10,11]

If we consider now the comparison of experimental results and theoretical calculations from the point of view of the influence of doubly ionized helium on the microfield distribution (see the Introduction), one can at least qualitatively explain most of the results of this comparison and in particular the very good agreement of our experiment with theory.[10,11] Here one should bear in mind that our experiment is performed at low electron temperatures (16 800–18 300 K) where the concentration of doubly ionized helium atoms was negligibly small. To prove this, we shall mention that with our plasma source it was not even possible to detect the He II 4686-Å line which was used in most other experiments for plasma diagnostic purposes (Table I). Therefore, our experiment is performed under plasma conditions (only singly ionized atoms present) which are closest to the conditions assumed in theoretical calculations. However, we should draw attention to three low-temperature experiments,[5–7] two of them performed in a shock tube[5,7] and one with a laser-produced plasma,[6] which do not fit into this simple explanation. In order to find the reasons for this inconsistency, we performed a critical analysis of the experiments and experimental procedure. We noticed that in both shock-tube experiments,[5,7] the plasma spectroscopic

TABLE II. Experimental results and estimated uncertainties.

Plasma parameters					
Electron density (10^{17} cm^{-3})	Temperature (K)	$\Delta\lambda_{1/2}$ (Å)	$\Delta\lambda_{AF}$ (Å)	I_F/I_A	I_V/I_A
0.54	16 900	18.1±1.0	9.2±0.4	0.85±0.04	0.57±0.04
0.79	17 300	25.6±1.2	12.2±0.6	0.90±0.04	0.61±0.03
1.32	17 800	40.2±1.5	18.2±1.0	1.00±0.02	0.69±0.02
1.91	18 300	54.8±2.0	23.4±1.0	1.04±0.02	0.74±0.02

observations were performed through 500-μm holes made in the expansion tube several millimeters in front of the reflector (see Figs. 1 and 3 of Refs. 5 and 7, respectively). It is very likely that the radiation emitted from the lower density plasma, which expanded through the hole, has distorted line-shape measurements. These influenced mostly the central part between the two investigated lines as seen in Fig. 4. The same effect most probably influenced considerably the measurements of the central structures of H_α and H_β lines as well.[7] At higher electron densities 3.4 and 4.4×10^{17} cm^{-3} in Ref. 5, the agreement with theory[5] is good. In our opinion, the experimental conditions in the shock tube were such that the intensity of the radiation from the inside of the tube was much higher than from outside in the vicinity of the observation holes, and in this way the agreement with theory was improved. In the case of the third low-temperature experiment by Hawryluk *et al.*,[6] we cannot offer an explanation for the good agreement with the high-temperature experiments (Figs. 1—4). However, we can only point out that the temperature measurements were crude in this particular experiment and that the authors themselves suggested that ". . . more accurate determinations of T_e should be performed before definitive evaluation of the present-day line shape theories."

IV. CONCLUSIONS

On the basis of the comparisons of our experiment with other experimental data and theoretical calculations (Figs. 1—4), we may conclude that the experimental conditions in most of the preceding experiments were such that reliable comparison with available theoretical calculations[10,11] cannot be made. Under our experimental conditions we approached closely the plasma conditions (only singly ionized atoms present in plasma) assumed in Refs. 10 and 11, and we found good agreement. Therefore, we suggest that theoretical calculations should be performed for each particular experimental plasma condition. On the other hand, the experiments should provide plasma composition data, which is not always an easy task. However, the final proof for our assumptions could only come from another set of theoretical calculations which would test the importance of doubly ionized atoms and would include all perturbing levels in the calculations of the shape of the He I 4471-Å line and its forbidden component.

ACKNOWLEDGMENTS

The authors gratefully acknowledge discussions with Dr. M. V. Popović and colleagues from the laser components division for their technical help.

[1]D. S. Lecrone, Astron. Astrophys. **11**, 387 (1971).
[2]B. J. O'Mara and R. W. Simpson, Astron. Astrophys. **19**, 167 (1972).
[3]G. Bekefi, C. Deutsch, and B. Yaakobi, in *Principles of Laser Plasmas,* edited by G. Bekefi (Wiley, New York, 1976); C. Fleurier, G. Coulaud, and J. Chapelle, Physica **100C**, 127 (1980); A. Piel and H. Richter, Z. Naturforsch. **38a**, 37 (1983); V. Helbig, in *Spectral Line Shapes, Vol. 3,* edited by F. Rostas (de Gruyter, Berlin, 1985).
[4]R. H. Nelson and A. J. Barnard, J. Quant. Spectrosc. Radiat. Transfer **11**, 161 (1971).
[5]J. R. Greig, L. A. Jones, and R. W. Lee, Phys. Rev. A **9**, 44 (1974).
[6]R. J. Hawryluk, G. Bekefi, and E. V. George, Phys. Rev. A **10**, 265 (1974).
[7]J. D. Hey and H. R. Griem, Phys. Rev. A **12**, 169 (1975).
[8]G. Baravian, J. Bretagne, J. Godart, and G. Sultan, Z. Phys. B **20**, 255 (1975).
[9]B. T. Vujičić and Lj. M. Ćirković, Fizika (Zagreb) **16**, 201 (1984).
[10]H. R. Griem, Astrophys. J. **154**, 1111 (1968).
[11]A. J. Barnard, J. Cooper, and L. J. Shamey, Astron. Astrophys. **1**, 28 (1969); Mem. Soc. Sci. Liege, Ser. 5 **17**, 89 (1969); A. J. Barnard (private communication).
[12]C. Deutsch, M. Sassi, and G. Coulaud, Ann. Phys. (N.Y.) **83**, 1 (1974).
[13]N. Konjević and W. L. Wiese, J. Phys. Chem. Ref. Data **5**, 259 (1976).
[14]W. L. Wiese, M. W. Smith, and B. M. Glennon, *Atomic Transition Probabilities, Vol. I,* Natl. Stand. Ref. Data Ser., Natl. Bur. Stand. (U.S.) Circ. No. 4 (U.S. GPO, Washington, D.C., 1966).